JOURNAL OF THERMOPHYSICS AND HEAT TRANSFER
Vol. 10, No. 4, October–December 1996

Heat Transfer to Annular Gas–Liquid Mixtures at Reduced Gravity

Larry B. Fore* and Larry C. Witte†
University of Houston, Houston, Texas 77204
and
John B. McQuillen‡
NASA Lewis Research Center, Cleveland, Ohio 44135

A series of fluid flow and heat transfer experiments was conducted for annular gas–liquid mixtures at reduced gravity aboard NASA's KC-135 aircraft. Air and two liquids, water and 50% aqueous glycerine, were used to produce a range of liquid Reynolds numbers from 1.4×10^2 to 1.4×10^4 in a 25.4-mm-i.d. tube. Pressure drop measurements compare reasonably well with the Lockhart and Martinelli and Wallis correlations. Film thickness measurements compare reasonably well with correlations derived from ground-based vertical annular flow data. The asymptotic Nusselt numbers for 50% glycerine compare well with a turbulent flat-film model, whereas the model overpredicts the water data. For both fluids at higher Reynolds numbers, the asymptotic Nusselt numbers follow a common dependence on Reynolds and Prandtl numbers, $Nu = ARe^nPr^{1/3}$.

Nomenclature

A = correlation constant
Cp = specific heat
D = tube diameter
f = friction factor
h = heat transfer coefficient
k = thermal conductivity
L = length
n = correlation power
q_w = wall heat flux
t^* = dimensionless time
U = velocity
u_* = friction velocity
X^2 = Lockhart and Martinelli parameter
x = axial direction
y = direction normal to tube wall
α = thermal diffusivity
Γ = mass flow per unit perimeter
ΔP = pressure drop
δ = film thickness
δ^+ = dimensionless film thickness
ε_h = eddy thermal diffusivity
η = two-phase heat transfer enhancement
μ = liquid absolute viscosity
ν = liquid kinematic viscosity
ρ = liquid density
τ = shear stress
ϕ_G = Lockhart and Martinelli gas multiplier
ϕ_L = Lockhart and Martinelli liquid multiplier

Subscripts
B = bulk
f = film
G = gas
IN = inlet
i = interfacial
L = liquid
N = Nusselt
OUT = outlet
S = superficial
w = wall

Received Dec. 26, 1995; revision received April 22, 1996; accepted for publication April 22, 1996.

*Postdoctoral Fellow, Department of Chemical Engineering; currently at Westinghouse Electric Corporation, West Mifflin, PA 15122.
†Professor, Department of Mechanical Engineering. Member AIAA.
‡Aerospace Engineer, Space Experiments Division.

Introduction

GAS–LIQUID mixtures occur in a number of situations relevant to ongoing and planned space operations. Some examples are the incidental boiling of cryogenic fluids, evaporative heating/cooling systems, and power generation systems. In these situations, knowledge of the phase distribution is important for the design of piping systems, separators, and other associated units. The prediction of heat transfer characteristics is of particular importance, since the design of such systems for space operations is inherently limited by size constraints.

It was recognized some time ago that predictions of normal-gravity two-phase flows could best be improved with flow regime-dependent models rather than purely empirical approaches. Following this reasoning, several studies have been performed to identify the flow regimes that occur under reduced-gravity and develop criteria for inter-regime transitions.[1–3] The three distinct regimes identified at reduced gravity are bubbly, slug, and annular, with transitions of bubbly–slug and slug–annular. Annular flow, where the liquid flows as a thin film along the tube wall and as droplets in a gas/vapor core, occurs over the widest range of gas and liquid flow rates. The largest frictional pressure gradients and heat transfer coefficients occur in annular flow, further increasing the need for good predictive methods.

Several two-phase convective heat transfer studies have been performed in a reduced gravity environment. Most of these studies have used a single component, either water or a refrigerant. Rite and Rezkallah[4] recently performed one of the only two-component studies, a sensible heating experiment for air–water flows in a 9.53-mm-i.d. tube. They compared heat transfer coefficients, averaged over a 35.6 cm heated length, with normal-gravity measurements obtained in the same apparatus for vertical upflow. Depending on flow conditions, the

heat transfer coefficients were higher or lower at reduced gravity vs normal gravity.

This article presents new heat transfer, pressure drop, and film thickness measurements for air–water and air–50% aqueous glycerine annular flows in a 25.4-mm-i.d. tube at reduced gravity. Local measurements of the heat transfer coefficient were made in a 56-cm-long heated section, located approximately 83 tube diameters downstream of the test section inlet. The measurements are compared to existing correlations and new relations are developed.

Experimental

Short durations of reduced gravity, less than 1% of Earth normal, are created aboard NASA's Zero-G KC-135 aircraft by a series of parabolic trajectories. The aircraft climbs and descends between altitudes of 7.6–10.6 km over the Gulf of Mexico, achieving reduced gravity for approximately 23 s at the crest of each trajectory. The data presented here were obtained aboard the KC-135 in October 1994 using a flow loop designed and constructed at NASA's Lewis Research Center and test sections designed and fabricated at the University of Houston.

Flow Loop

The layout of the flow loop used in these experiments is shown in Fig. 1. A more complete description is provided elsewhere.[5] Liquid was displaced in the cylindrical feed tank by an air-driven piston and metered through turbine flow meters. Air was supplied from compressed air bottles and metered through orifice meters, entering the test section through a gas–liquid mixer. Liquid entered the test section as a thin film through an annular slot in the gas–liquid mixer. The mixer was designed to create an annular configuration at the inlet, which helps to minimize the required flow development length. After flowing through the test section, the liquid and gas exited into a separator, where the gas was vented off and the liquid collected for recycle in the periods between trajectories.

The adiabatic sections between the mixer and the heated section and between the heated section and the outlet were constructed of 25.4-mm-i.d. clear acrylic tubing. The heated section was constructed of 25.9-mm-i.d. copper tubing, with nylon end-flanges machined to make a smooth transition to the acrylic tubing i.d. Two pressure taps for the pressure gradient measurement were located upstream of the heated section at locations 1.33 and 1.96 m from the inlet. This provided an average development length of 65 tube diameters for the pressure gradient measurement. Since the liquid and gas were injected in an annular configuration, this length should be adequate for an estimate of the fully developed pressure gradient. A film thickness and void fraction probe, separated axially by 50 mm, were located at the second pressure tap. The heated test section was located 2.11 m from the inlet and had an overall length of 0.73 m, including the adiabatic end-flanges. The adiabatic length was chosen to minimize the evaporative heat flux, which is significant near the mixer where the air is dry. The exit section leading to the separator was 0.51 m long.

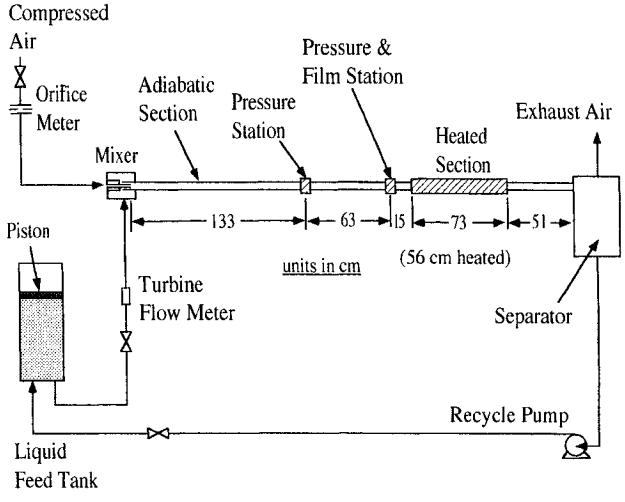

Fig. 1 KC-135 gas–liquid flow loop.

Test Section and Measuring Techniques

The axial pressure gradient was estimated between the two pressure stations with two Druck PDCR 820, 1-psi-range, pressure transducers. Pressure reference lines from each transducer were connected in common to the test section outlet to keep the measured pressures within the 1-psi (6900 Pa) measurable range. Before each run, liquid was purged through the pressure taps into the test section to remove any trapped air bubbles. The film thickness and void fraction conductance probes consisted of parallel pairs of 76-μm-diam 13% Rh–Pt wires, stretched across the tube diameter and separated by 3 mm. The film thickness wires were insulated over half of the i.d. to restrict the measurement to one side of the tube, while the void fraction wires were bare. The conductance between the wires was measured with a circuit described in detail by Lacy and Dukler.[6] The output of the circuit is directly proportional to the thickness of the liquid film between the uninsulated portions of the wires, when compensated for temperature-dependent conductivity variations. This compensation was performed by normalization with the circuit output for full pipe flow conditions. The void fraction probe measures twice the film thickness for symmetric conditions, or averages the film thickness on opposite sides of the tube diameter for nonsymmetric conditions. This represents a more accurate measurement of the mean film thickness, since the accuracy of the probes increases with the amount of liquid between the wires, but does not provide the same local dynamic information as the film thickness probe. Because of the greater accuracy, the mean film thicknesses used in this article were obtained with the void fraction probe.

The heated section is depicted in detail in Fig. 2. The copper tube, with a wall thickness of 1.27 mm, was nickel-plated and grounded to reduce interference with the conductance probes. The outside of the tube was wrapped with three 36-Ω (nominal) etched-foil nickel resistance heaters, connected in parallel to 60-Hz-ac power aboard the aircraft. The heaters covered all but a 1-cm strip along the length of the copper tube. The wall temperature profile was measured in that strip with eight 50-Ω nickel resistance temperature detectors (RTDs), which were cemented to the tube o.d. Vinyl tape was used to secure the heaters and cover the RTDs, and an acrylic box enclosed the heater-tube assembly, serving both as a mount for electrical connections and as insulation against ambient heat loss. An Analog Devices 2B31J strain-gauge circuit was used to measure the RTD resistances. The entrance bulk temperature was estimated with a nickel RTD mounted inside the nylon flange at the heater entrance. Another RTD was mounted in a 7-deg expansion section downstream of the heater. The expansion was designed to decrease the amplitude of large disturbance waves and lessen wave-dependent fluctuations in fluid temperature, providing an estimate of the exit bulk fluid temperature.

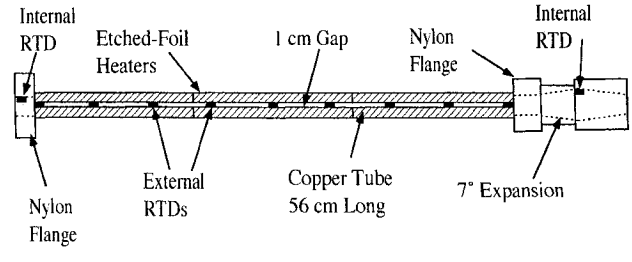

Fig. 2 Schematic of heated test section.

The two pressures, film thickness, eight wall temperatures, and inlet and outlet temperatures were collected at 1 kHz. Three acceleration components at two positions along the flow loop were also collected at 1 kHz. Miscellaneous test section temperatures, pressures, and flow rates were collected at 1 Hz.

Temporal Response

Because of the transient nature of this experiment, where sometimes nearly all of the reduced-gravity period is required to reach quasisteady state, careful examination of the measured time series is required to obtain meaningful information. Using the measured acceleration components, data corresponding to poor gravity levels were eliminated from consideration. When acceptable gravity levels, on the order of 0.01 g, were present, the time histories of pressure and film thickness reached steady values 2–5 s after the flow was initiated. The wall temperatures along the heated section, however, required a much longer time to reach steady values, a problem that has been addressed previously by Rite and Rezkallah[4] for similar experiments. A simple analysis was performed to estimate the required time to reach steady state. Assuming a wave-free laminar flow, the velocity profile in the film was estimated with

$$u = (\tau/\mu)y \tag{1}$$

where the distance y is measured from the tube wall and τ is a constant shear stress over the film thickness. Using this approximation for the velocity profile, the two-dimensional transient convection–conduction equation

$$\frac{\partial T}{\partial t} + u\frac{\partial T}{\partial x} = \alpha\frac{\partial^2 T}{\partial y^2} \tag{2}$$

was solved with the conditions of uniform wall heat flux, negligible heat flux at the interface, and a uniform temperature profile at the heater entrance. The assumption of negligible interfacial heat transfer is based on the placement of the heated section where evaporation can be neglected. From this analysis, the time required to reach steady state at various positions along the heated section was estimated.

For the 56-cm heated length and flow conditions typical of the current experiments, the time required is approximately $t^* = \delta^2/\alpha$, the first-order time constant. For a laminar annular flow this represents the minimum time required to reach steady state, since a finite time is required for the heaters and tube to reach thermal equilibrium. Typical of these experiments, all of the temperatures except the two farthest downstream reached steady values by the end of the 20-s recording period. An example of the temporal response for the wall temperatures is shown in Fig. 3. The crossover of wall temperature time series occurs because wall temperatures farther downstream take longer to reach steady values. The response is better for the water runs, for which the time constant is on the order of a few seconds. For the 50% glycerine experiments, the time constants are significantly longer, sometimes exceeding the 20-s period. Even for these cases, appropriate data reduction can be used to estimate the asymptotic heat transfer coefficients.

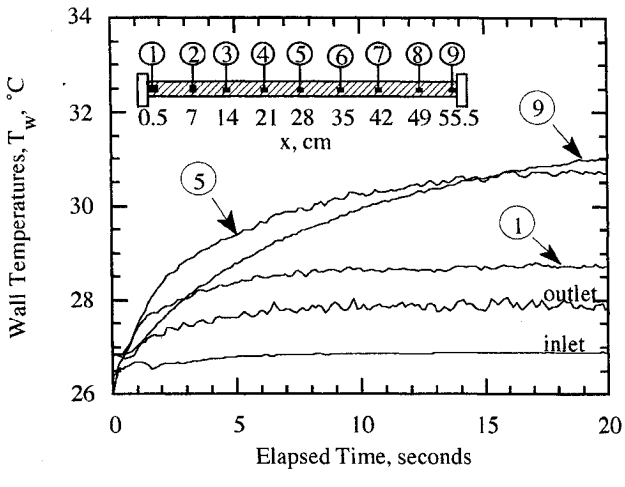

Fig. 3 Test section temperatures during one trajectory for water at $Re_L = 1.66 \times 10^4$ and $Re_G = 9.4 \times 10^3$.

Calculation of Heat Transfer Coefficients

Using time series as shown in Fig. 3, the steady-state wall temperatures were estimated for each run by averaging over the last 2–5 s of the recording period, at which the wall temperatures were at or approaching asymptotic values. Because the temporal response depends on flow conditions, the averaging period varied from run to run. The local bulk temperature was estimated from two sources, interpolation between the measured inlet and outlet temperatures as

$$T_B = T_{IN} + [(T_{OUT} - T_{IN})/L]x \tag{3}$$

and from an enthalpy balance on the liquid as

$$T_B = T_{IN} + (q_w x/\Gamma CP) \tag{4}$$

For significant droplet entrainment, these two methods for estimating the bulk temperature could differ, depending on how rapidly enthalpy is exchanged between the liquid film and droplets through entrainment and deposition. However, the two methods agree particularly well for these experiments, and so for convenience, the temperature obtained with Eq. (4) was used to estimate the local heat transfer coefficient $h = q_w/(T_w - T_B)$.

Depending on flow conditions, the wall and bulk temperatures vary widely among experiments. To aid in the analysis of the asymptotic heat transfer coefficients, the temperatures and axial distance were placed in dimensionless forms based on the laminar flat-film analysis. Local heat transfer coefficients were computed in dimensionless form, based on the laminar Nusselt film thickness,

$$\delta_N = (Re\mu^2/2\rho\tau)^{1/2} \tag{5}$$

where the shear stress was estimated with an axial momentum balance as $\tau = -(D/4)\Delta P/L$. The dimensionless heat transfer coefficient $h\delta_N/k$ is essentially the Nu based on the thickness of a flat laminar film instead of the actual measured thickness. While the actual thickness is larger for turbulent films, the Nusselt thickness was used to provide a uniform treatment for all conditions and for comparison with the theoretical laminar solution. The laminar solution can be used as a reference for the magnitude of the heat transfer coefficient and for the length of the thermal entry region, thus its usefulness in estimating the asymptotic heat transfer coefficients.

Several examples of dimensionless heat transfer coefficients calculated with the laminar Nusselt film thickness are shown in Fig. 4. The thermal entry-length for run 658 is shorter than that predicted from laminar, flat-film theory, because of the larger heat transfer coefficient, wave motion, and film turbulence. The asymptotic heat transfer coefficient is fairly easy to interpret in this case, since the wall temperatures reached steady values within the experimental period and the local dimensionless heat transfer coefficient is not changing at the heater exit. The asymptotic coefficient is significantly larger than the laminar value, which is expected since $Re = 9.57 \times 10^3$. Similarly, the asymptotic heat transfer coefficient is easily estimated from run 690 by averaging over the measurements downstream of the thermal entry region. In this case, $Re = 1.55 \times 10^3$ and the asymptotic coefficient is much closer to the laminar value. The analysis is more difficult for run 660. The wall temperatures farthest downstream did not reach

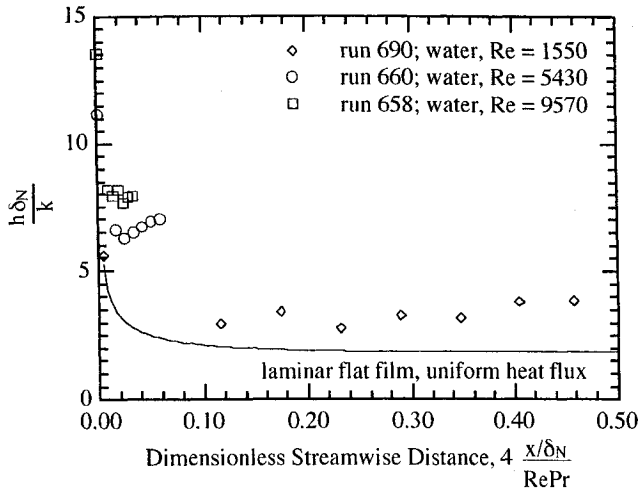

Fig. 4 Dimensionless heat transfer coefficients along heated section.

steady values, thus the computed coefficients at the heater exit are larger than the asymptotic value. For cases similar to run 660, the asymptotic heat transfer coefficients were estimated by averaging the steady measurements downstream of the thermal entry region. This typically included all locations except the farthest upstream and two farthest downstream.

Error Analysis

There are a number of identifiable sources of error in these experiments, besides instrument and calibration errors. These include a lack of flow development, nonuniform wall heat flux, and evaporation at the interface. The flow development length in annular flow depends on the dynamic interaction between entrainment and deposition rates, which are approximately equal when the flow is fully developed. The expansion of the gas under large pressure gradients, which occurs primarily in small-diameter tubes at large mass fluxes, is one source for a lack of flow development. As the gas accelerates along the tube length, the entrained fraction and frictional pressure gradient increase, which can lead to very long development lengths.[7] In these experiments, the largest pressure gradients are on the order of 2000 Pa/m, which corresponds to a velocity increase of only 2%/m at atmospheric pressure. Under similar flow and pressure gradient conditions in a 5.08-cm vertical tube on the ground, fully developed annular flow was attained at 65 tube diameters from the feed, as determined with detailed entrainment measurements.[8] Based on the mechanism of gas acceleration, the flow is considered within 2% of full development for both the pressure gradient and heat transfer measurements.

The time-averaged wall heat flux was determined to be uniform with falling-film experiments on the ground.[9] Nylon's low thermal conductivity makes the end-flanges effective insulators, so that any axial conduction into them can be neglected. Evaporation at the interface is a significant effect near the gas–liquid mixer, where dry air contacts the liquid film. Based on an analysis with the Gilliland and Sherwood[10] mass transfer correlation, the heater was placed at a position downstream where the evaporative heat flux should be less than 2% of the input wall heat flux.

Uncertainties in the measured and calculated quantities were estimated with the Kline and McClintock[11] method, assuming sampling periods long enough to obtain stationary means. The relative uncertainty in the asymptotic heat transfer coefficient is dominated by the uncertainty in the wall heat flux, ±10%, which is the sum of the uncertainty in power input and the effect of evaporation. The 1-cm unheated strip had no effect on falling-film experiments, and so it is neglected here as a source of uncertainty. The relative uncertainties of the liquid Reynolds numbers ($Re = 4\Gamma/\mu$) are ±2 and ±5% for water and 50% glycerine, respectively, based on errors in the estimated viscosities and measured flow rates. Similarly, the relative uncertainties of the liquid Prandtl numbers ($Pr = Cp\mu/k$) are ±2 and ±4%, based on errors in the estimated viscosities and thermal conductivities. The relative uncertainty in the gas Re was estimated as ±9%, based on errors in flow rate and pressure.

The uncertainty in the pressure gradient was estimated as ±150 Pa/m, based on the rated ±1% accuracy of the pressure transducers and distance between pressure taps. For the majority of the present experiments, the measured pressure gradient fell in the range 1000–2000 Pa/m, and so the typical relative uncertainty is smaller than ±15%. Other experimental conditions, such as the presence of bubbles in the pressure taps and insufficient sampling time, may increase the uncertainty in the measured pressure gradient. The uncertainty associated with the film thickness measurement is approximately ±0.05 mm, based on the accuracy of the calibration and compensation for conductivity changes. For the current conditions, the associated relative uncertainty is typically less than ±10%.

Results

Two liquids, water and 50% aqueous glycerine, were used in these experiments with an average wall heat flux of 18,700 W/m^2. The physical properties of the two fluids produce nominal Pr of 6 and 36, respectively, at 20°C. The Re and Pr were calculated with physical properties evaluated at the exit bulk liquid temperature and the wall Pr was calculated with physical properties evaluated at the exit wall temperature. The liquid Re lie primarily in the laminar–turbulent transition region for full pipe flows, but thin films are generally considered turbulent for $Re > 1600$. The minimum superficial gas velocity is approximately 5 m/s, which lies near the upper end of the slug–annular transition determined in Bousman's[5] flow pattern study, and extends to approximately 25 m/s.

Pressure Gradient and Film Thickness

The Lockhart and Martinelli[12] (L–M) correlation is used first in the analysis of the measured pressure gradient, $\Delta P/L$. The L–M gas multiplier, $\phi_G^2 = \Delta P/\Delta P_G$, is plotted vs the L–M parameter, $X^2 = \Delta P_L/\Delta P_G$, in Fig. 5. The single-phase pressure drops, ΔP_L and ΔP_G were calculated with the friction factors, $f = 16/Re$ and $f = 0.08/Re^{1/4}$, for $Re < 2.0 \times 10^3$ and $Re > 2.0 \times 10^3$, respectively. Conditions for which the estimated uncertainty of 150 Pa/m exceeded 15% of the measurement are not included in this figure. The agreement is adequate with the Chisholm and Laird[13] equation,

$$\phi_G^2 = 1 + 20X + X^2 \tag{6}$$

which has been previously established by Bousman. Even after removing conditions with greater than 15% uncertainty, some scatter remains. Bousman found agreement within ±15% for a smaller diameter (12.7-mm) tube, for which the measured pressure drop was significantly larger.

The Wallis[14] correlation uses the ratio of mean film thickness to tube diameter as a measure of film roughness. In this relation, the friction factor calculated with the superficial gas velocity

$$f_i = -\frac{D}{2}\frac{\Delta P/L}{\rho_G U_{GS}^2} \tag{7}$$

follows the dependence

$$f_i = 0.005[1 + 300(\delta/D)] \tag{8}$$

Figure 6 displays the friction factors calculated according to Eq. (7) along with the Wallis correlation [Eq. (8)]. Like the

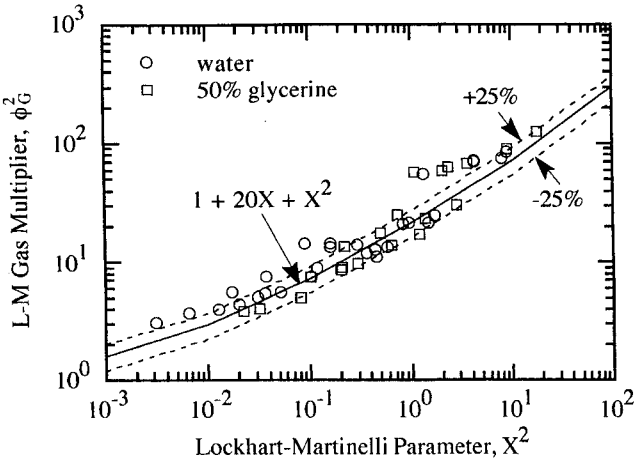

Fig. 5 Comparison of measured pressure gradient with the L–M[12] correlation.

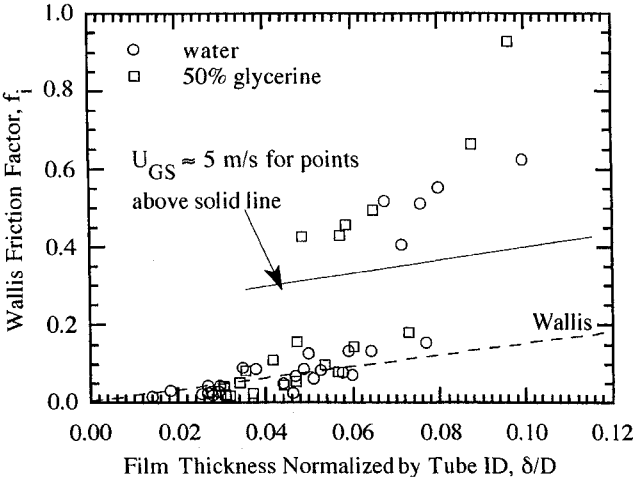

Fig. 6 Comparison of measured friction factors with the Wallis[14] correlation.

L–M comparison, measurements with uncertainties greater than 15% are not included. The points lying below the solid line follow this correlation reasonably well, showing scatter above and below the Wallis values. The points that lie above the solid line, which do not in any sense follow this dependence, correspond to gas velocities around 5 m/s. Although these data runs were annular in the sense that liquid did not bridge the tube diameter, this gas velocity lies at the upper end of the slug-to-annular transition and would not necessarily be expected to follow the same behavior as annular flows at higher gas velocities. A similar behavior exists for Earth-normal vertical upward flows in a range of gas velocities just above the flooding condition. A significant source of error for these particular measurements may be a requirement for longer sampling periods to achieve stationary mean values.

The laminar model for film thickness, Eq. (5), applies in general for Re less than about 1.6×10^3. For larger Re, the film thickness increases more rapidly with Re, because of the increased waviness and turbulence. Several correlations have been proposed for the film thickness in annular flow at Earth-normal gravity. The film thickness is correlated in terms of the friction velocity, $u_* = \sqrt{\tau/\rho}$ as

$$\delta^+ = \delta u_*/\nu = f(Re) \tag{9}$$

Strictly, the correlation [Eq. (9)] requires knowledge of the film flow rate, which is the overall flow rate minus the entrained droplet flow rate. However, for the purpose here, all of the liquid is assumed to travel in the film and the Re is assigned an additional uncertainty of 10%. The measured mean film thickness, normalized in this way, is plotted in Fig. 7. Although there is significant scatter, the points do follow a general trend consistent with Bousman's[4] findings in a 12.7-mm-i.d. tube. Bousman's[5] fit

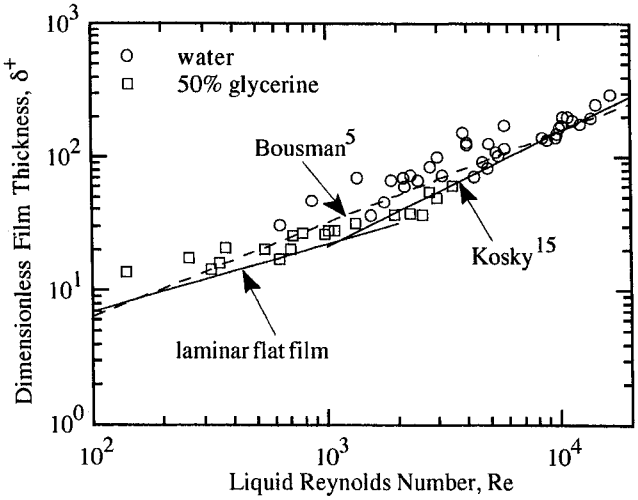

Fig. 7 Correlation of experimental film thickness with liquid *Re*.

$$\delta^+ = 0.265 Re^{0.695} \tag{10}$$

the laminar equation

$$\delta^+ = \sqrt{Re/2} \tag{11}$$

and Kosky's[15] relation

$$\delta^+ = 0.0504 Re^{7/8} \tag{12}$$

are included for comparison. A significant number of points for $Re > 1.6 \times 10^3$ agree reasonably well with the Kosky relation, while the agreement with the laminar relation for $Re < 1.6 \times 10^3$ is not quite as good. Some of the scatter is caused by the conditions near $U_{GS} = 5$ m/s, where the pressure drop is larger than that expected for typical annular flows. Bousman's low-Re data agree more closely with the laminar model, which may be because of random or bias errors in the current set of data. Andreussi and Zanelli[16] found very good agreement with the laminar and Kosky equations for a large number of gas–liquid downflow experiments. These reduced-gravity experiments are similar in many respects to shear-stress-dominated vertical annular downflows; i.e., the absence of flooding phenomena, axisymmetry, and a diminished effect of gravity. Thus, the measured film thickness should be expected to follow correlations such as Kosky's, which was developed from shear-driven annular flow data.

Heat Transfer Coefficients

Several empirical methods for correlating the two-phase heat transfer coefficient have been proposed. These differ significantly from the more mechanistic approach of correlating film thickness-based Nu with Re and Pr, but the generality of empirical methods can allow extension to other flow patterns. A typical way of presenting two-phase heat transfer coefficients is with the two-phase enhancement $\eta = h/h_L$, where h_L is a single phase heat transfer coefficient measured or computed at the same liquid Re and Pr. This enhancement has been correlated with void fraction,[17,18] the gas-to-liquid velocity ratio,[19] and the L–M liquid multiplier $\phi_L^2 = \Delta P/\Delta P_L$.[20,21]

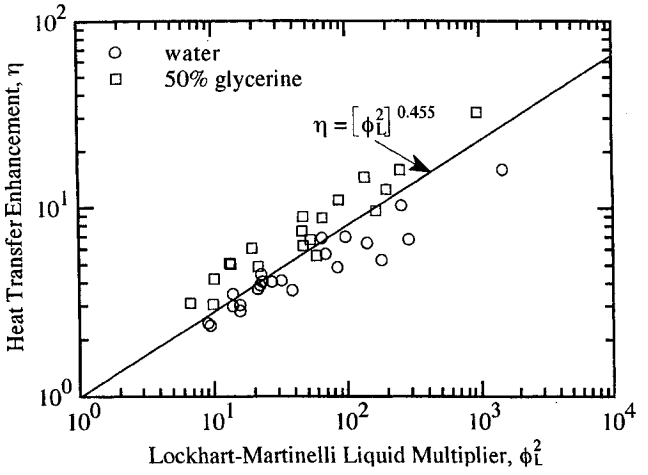

Fig. 8 Comparison of two-phase heat transfer enhancement with the Vijay et al.[21] correlation for annular flow.

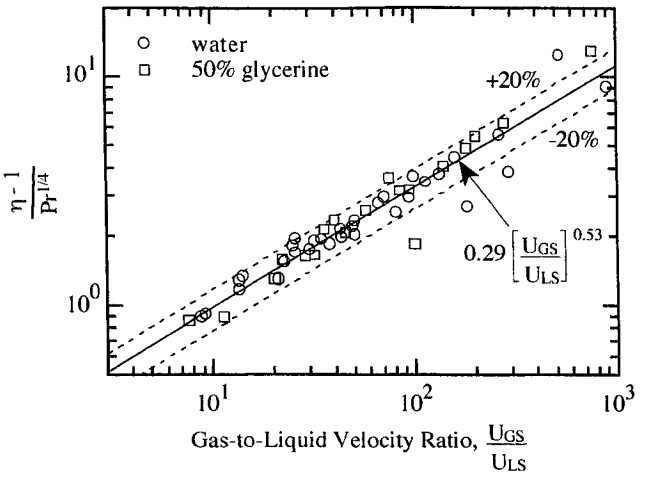

Fig. 9 Correlation of heat transfer enhancement with gas-to-liquid velocity ratio.

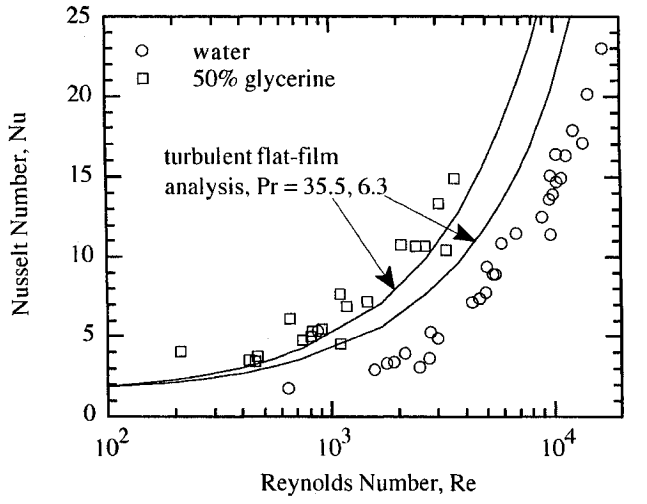

Fig. 10 Comparison of measured *Nu* with turbulent flat-film analysis using the universal velocity profile.

Vijay et al.[21] treated individual flow patterns in correlating a large set of ground-based data. The reduced-gravity heat transfer enhancements measured in this work are plotted vs ϕ_L^2 in Fig. 8, with the Vijay et al. correlation included for comparison. The Sieder and Tate[22] turbulent correlation was used to calculate the single-phase heat transfer coefficients. The agreement is satisfactory for about half the water runs at smaller heat transfer enhancements and for some of the 50% glycerine runs. In general, the data show no clear difference from the Vijay et al. correlation derived from normal-gravity annular flows. A form similar to Rezkallah and Sims' [19] laminar correlation, with a difference in the power of the *Pr*, represents the data well. The current data are plotted in the form of this correlation:

$$\eta = 1 + A(U_{GS}/U_{LS})^n Pr^{1/4} \tag{13}$$

in Fig. 9. Most of the data lie within ±20% for constant values of $A = 0.29$ and $n = 0.53$. This is a purely empirical relation, with no theoretical justification for the power on the *Pr*, although the gas-to-liquid velocity ratio can be viewed as representative of the increase in liquid velocity caused by the gas phase.

As opposed to empirical approaches, the mechanistic approach of correlation with the film thickness should provide more general relations. There is an established theory for the heating of purely laminar films, and the use of eddy diffusivity or other models for turbulent heat transfer allows the extension of this theory to turbulent films. Figure 10 displays *Nu* calculated with the measured asymptotic heat transfer coefficient and the experimental film thickness, $Nu = h\delta/k$, vs the liquid *Re*. The film thickness was adjusted slightly according to Eqs. (11) and (12), to compensate for the difference in temperature between the heated section and the adiabatic section where the film thickness measurement was performed. This adjustment results in a slightly thinner film inside the heated tube, because of the decreased liquid viscosity. The factor $(Pr/Pr_w)^{1/4}$ is included to account for physical property variations across the thermal boundary layer.[23]

Two theoretical curves are included in Fig. 10 for comparison with the experimental measurements. The *Nu* represented by these curves were calculated with the steady turbulent convection–conduction equation

$$u\frac{\partial T}{\partial x} = \frac{\partial}{\partial y}\left[(\alpha + \varepsilon_h)\frac{\partial T}{\partial y}\right] \tag{14}$$

with conditions of a uniform wall heat flux and negligible heat transfer at the interface. The *u* velocity and eddy thermal diffusivity were approximated by the universal velocity profile, assuming the equality of eddy thermal and momentum diffusivities. This is an established approach that has been applied quite successfully to evaporation and condensation problems, and is described in some detail by Butterworth[24] and Shock,[25] among others. Analysis with this technique results in the theoretical laminar Nusselt number, $Nu = 15/8$, at low *Re*. Above a certain *Re*, the *Nu* increases above the theoretical laminar value. As the *Pr* increases, the value of that critical *Re* decreases. This is consistent with data from the literature and with the current set of data, although in reality some of the increase above the flat-film laminar value is because of interfacial waviness. The two curves shown in Fig. 10 correspond to mean *Pr* for the water ($Pr = 6.3$) and 50% glycerine ($Pr = 35.5$) experiments. The 50% glycerine data agree reasonably well with the turbulent flat-film model, but the water data are significantly lower than the prediction.

Part of the difference between the water data and the turbulent flat-film model may be the uncertainty in the measured heat transfer coefficient, although the uncertainty in the 50% glycerine data is greater because of larger time constants. Another reason could be the presence of significant droplet entrainment, which would shift the data to *Re* less than those based on the feed flow rate. However, the measured film thicknesses do agree fairly well with correlations at the same *Re*. A very plausible reason may be that the eddy thermal diffusivity differs significantly from that derived from the universal

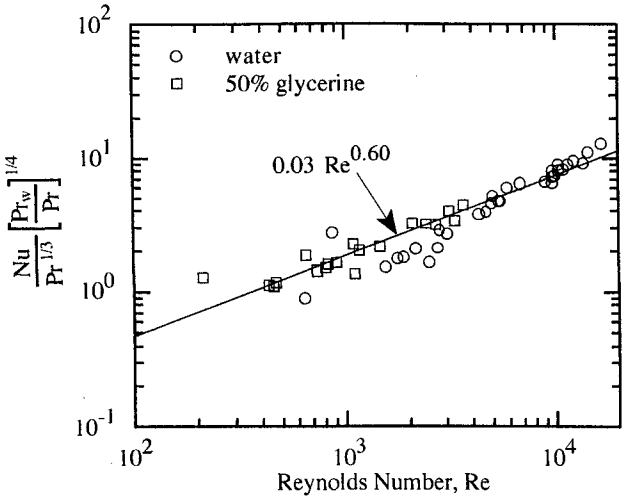

Fig. 11 Correlation of experimental *Nu*.

velocity profile, particularly at the gas–liquid interface. No allowance is made in this model for the dampening of eddies at the interface. In fact, eddy–viscosity modeling in thin film flows has been a research topic for quite some time. The thermal boundary layer is thinner for higher *Pr*, so overprediction of ε_h at the interface could affect the results for water and not for 50% glycerine. This is one way to explain why the 50% glycerine data compare well with the model while the water data does not.

For most conditions, with the exception of low-*Re* data, the differences in *Nu* for the two fluids are adequately represented by the factor $Pr^{1/3}$. The asymptotic *Nu* correlated in this fashion are shown in Fig. 11. The lower *Re* data for water deviate from the common dependence of the two fluids, since those data approach the laminar flat-film value as shown in Fig. 10. The higher *Re* data for each fluid correlate according to

$$Nu = ARe^n Pr^{1/3} \tag{15}$$

with the constants $A = 0.03$ and $n = 0.60$. Most of the higher *Re* data follow this relationship, but more experimental data are clearly needed to improve the uncertainty in this equation, as well as the uncertainty in Eq. (13).

Summary

Pressure gradient, film thickness, and heat transfer measurements have been made for annular gas–liquid flows of air–water and air–50% glycerine under reduced gravity conditions. The pressure gradient agrees fairly well with a version of the L–M correlation and with the Wallis correlation, but the measured film thickness deviates from published correlations at lower *Re*. The *Nu* for 50% glycerine follow a turbulent flat-film model reasonably well, whereas the model overpredicts the *Nu* for water. At larger *Re*, the *Nu* for both fluids follow the relation, $Nu = ARe^n Pr^{1/3}$, but more experimental data in a reduced gravity environment are needed to increase the confidence in the estimated constants, *A* and *n*.

Acknowledgments

This research was supported by the NASA Lewis Research Center under Grant NAG3-510. Special thanks go to the Lewis team of G. Fedor, S. Fisher, T. Lorik, and M. Shoemaker, and to R. Mate at the University of Houston.

References

[1]Dukler, A. E., Fabre, J. A., McQuillen, J. B., and Vernon, R., "Gas-Liquid Flow at Microgravity Conditions: Flow Patterns and Their Transitions," *International Journal of Multiphase Flow*, Vol. 14, No. 4, 1988, pp. 389–400.

[2]Zhao, L., and Rezkallah, K. S., "Gas-Liquid Flow Patterns at Microgravity Conditions," *International Journal of Multiphase Flow*, Vol. 19, No. 5, 1993, pp. 751–763.

[3]Bousman, W. S., and Dukler, A. E., "Ground Based Studies of Gas-Liquid Flows in Microgravity Using Lear Jet Trajectories," AIAA Paper 94-0829, Jan. 1994.

[4]Rite, R. W., and Rezkallah, K. S., "Heat Transfer in Two-Phase Flow Through a Circular Tube at Reduced Gravity," *Journal of Thermophysics and Heat Transfer*, Vol. 8, No. 4, 1994, pp. 702–708.

[5]Bousman, W. S., *Studies of Two-Phase Gas-Liquid Flow in Microgravity*, Ph.D. Dissertation, Univ. of Houston, Houston, TX, 1994; also NASA CR-195434, Jan. 1995.

[6]Lacy, C. E., and Dukler, A. E., "Flooding in Vertical Tubes—I. Experimental Studies of the Entry Region," *International Journal of Multiphase Flow*, Vol. 20, 1994, pp. 219–233.

[7]Hewitt, G. F., and Hall-Taylor, N. S., *Annular Two-Phase Flow*, Pergamon, Oxford, England, UK, 1970.

[8]Fore, L. B., and Dukler, A. E., "Droplet Deposition and Momentum Transfer in Annular Flow," *AIChE Journal*, Vol. 41, No. 9, 1995, pp. 2040–2046.

[9]Fore, L. B., and Witte, L. C., "Roll-Wave Effects on the Heating of Viscous Liquid Films," *Proceedings of the 30th National Heat Transfer Conference*, HTD-Vol. 314, American Society of Mechanical Engineers, New York, 1995, pp. 23–30.

[10]Gilliland, E. R., and Sherwood, T. K., "Diffusion of Vapors into Air Streams," *Industrial and Engineering Chemistry*, Vol. 26, No. 5, 1934, pp. 516–523.

[11]Kline, S. J., and McClintock, F. A., "Describing Uncertainties in Single Sample Experiments," *Mechanical Engineering*, Jan. 1953, pp. 3–8.

[12]Lockhart, L. W., and Martinelli, R. C., "Proposed Correlation of Data of Isothermal Two-Phase, Two Component Flow in Pipes," *Chemical Engineering Progress*, Vol. 45, No. 1, 1949, pp. 39–48.

[13]Chisholm, D., and Laird, A. D. M., "Two-Phase Flow in Rough Tubes," *Transactions of the American Society of Mechanical Engineers*, Vol. 80, 1958, pp. 276–286.

[14]Wallis, G. B., *One Dimensional Two Phase Flow*, McGraw–Hill, New York, 1969.

[15]Kosky, P. G., "Thin Liquid Films Under Simultaneous Shear and Gravity Forces," *International Journal of Heat and Mass Transfer*, Vol. 14, No. 8, 1971, pp. 1220–1224.

[16]Andreussi, P., and Zanelli, S., "Downward Annular and Annular-Mist Flow of Air-Water Mixtures," *Two-Phase Mass, Momentum, and Heat Transfer in Chemical Process and Engineering Systems*, Vol. 2, Hemisphere, Washington, DC, 1979, pp. 303–314.

[17]Kudirka, A. A., Grosh, R. J., and McFadden, P. W., "Heat Transfer in Two-Phase Flow of Gas-Liquid Mixtures," *Industrial and Engineering Chemistry Fundamentals*, Vol. 4, No. 3, 1965, pp. 339–344.

[18]Dorresteijn, W. R., "Experimental Study of Heat Transfer in Upward and Downward Two-Phase Flow of Air and Oil Through 70-mm Tubes," *Proceedings of the 4th International Heat Transfer Conference*, Vol. 5, Paper B5.9, Hemisphere, Washington, DC, 1970, pp. 1–11.

[19]Rezkallah, K. S., and Sims, G. E., "An Examination of Correlations of Mean Heat-Transfer Coefficients in Two-Phase Two-Component Flow in Vertical Tubes," *AIChE Symposium Series*, Vol. 83, No. 257, 1987, pp. 109–114.

[20]Fried, L., "Pressure Drop and Heat Transfer for Two-Phase, Two-Component Flow," *Chemical Engineering Progress Symposium Series*, Vol. 50, No. 9, 1954, pp. 47–51.

[21]Vijay, M. M., Aggour, M. A., and Sims, G. E., "A Correlation of Mean Heat-Transfer Coefficients for Two-Phase Two-Component Flow in a Vertical Tube," *Proceedings of the 7th International Heat Transfer Conference*, Vol. 5, Hemisphere, Washington, DC, 1982, pp. 367–372.

[22]Sieder, E. N., and Tate, G. E., "Heat Transfer and Pressure Drop of Liquids in Tubes," *Industrial and Engineering Chemistry*, Vol. 28, No. 12, 1936, pp. 1428–1436.

[23]Gimbutis, G., "Heat Transfer of a Turbulent Vertically Falling Film," *Proceedings of the 5th International Heat Transfer Conference*, Vol. 2, 1978, pp. 85–89.

[24]Butterworth, D., "An Analysis of Film Flow and Its Applications to Condensation in a Horizontal Tube," *International Journal of Multiphase Flow*, Vol. 1, No. 5, 1974, pp. 671–682.

[25]Shock, R. A. W., "Convective Heat Transfer in Annular Flow," *Two-Phase Flow and Heat Transfer*, Oxford Univ. Press, Oxford, England, UK, 1977, pp. 170–199.